Journal of Hazardous Materials 187 (2011) 182–189

Contents lists available at ScienceDirect

Journal of Hazardous Materials

journal homepage: www.elsevier.com/locate/jhazmat

Fixed-bed column study for Cu^{2+} removal from solution using expanding rice husk

Xuegang Luo*, Zaifang Deng, Xiaoyan Lin, Chi Zhang

Engineering Research Center of Biomass Materials of Education Ministry, Southwest University of Science and Technology, Mianyang, Sichuan 621010, China

ARTICLE INFO

Article history:
Received 24 September 2010
Received in revised form
27 December 2010
Accepted 4 January 2011
Available online 12 January 2011

Keywords:
Expanding rice husk
Cu^{2+}
Breakthrough curve
Equilibrium uptake

ABSTRACT

This paper deals with removal of copper ions from solution by raw rice husk (RRH) and expanding rice husk (ERH). Different column design parameters like bed depth, flow rate and initial copper concentration were investigated. It was found that the equilibrium uptake ($q_{eq(exp)}$) of the ERH and RRH increased with increase in initial copper concentration but decreased with increase in flow rate and bed depth, respectively. The higher adsorption capacity and longer breakthrough time were observed for ERH in comparison with RRH, under the same conditions. Compared to coconut-shell activated carbon (C-AC), ERH was also found more effective in removing Cu^{2+}. 0.01 mol L^{-1} HCl solution was used for desorption of column which was prior to absorb copper ion, and 0.01 mol L^{-1} NaOH solution was used for re-activation. Column regeneration and reuse studies were conducted for adsorption–desorption cycle.

1. Introduction

The copper is essential and healthy to humans. However, like all heavy metals, it is potentially toxic as well. The excessive intake of copper results in its accumulation in the liver and produces gastrointestinal problems, kidney damage, anemia and continued inhalation of copper-containing sprays which is linked with an increase in lung cancer among exposed workers [1–6]. Therefore, it is important to eliminate traces of copper from drinking water, or to remove copper from wastewater before they are discharged into receiving bodies.

Various treatment techniques have been employed to eliminate or reduce copper in wastewater including precipitation, adsorption, ion exchange and reverse osmosis [7–9]. As of now, adsorption by activated carbon is accepted to be the best available technology for the reduction of heavy metals, except that its manufacturing cost is quite high [10]. Hence, a search is on worldwide for a low-cost alternative. Research in recent years has indicated that some natural biomaterials including agricultural products and by-products can accumulate high concentration of heavy metals [11–14]. Agricultural products and by-products have been reported to be effective in removing copper. Rice husk, an abundant agricultural product, is capable of removing heavy metals and can be considered as an efficient and low-cost adsorbent for heavy metals. In recent years, attention has been taken on the utilization of unmodified or modified rice husk as a sorbent for the removal of pollutants [15,16].

In this paper, the adsorption characteristics of Cu^{2+} on raw rice husk (RRH) and expanding rice husk (ERH) are studied in fixed bed column with varying parameters of inlet concentration, flow rate and bed depth.

2. Materials and methods

2.1. Preparation of adsorbent

2.1.1. RRH

Crushed rice husk was obtained from Deyang Haitian high-tech materials Manufacturing Co., Ltd. Before pretreatment, it was washed with distilled water for several times to remove the impurities. This rice husk was referred hereinafter to as raw rice husk (RRH).

2.1.2. Preparation and characterization of ERH

3–5 wt% sodium carbonate agent which helps expansion of raw rice husk is added into high-performance electromagnetic induction heat extruder. Feed temperature at 80–110 °C and discharge temperature at 250–300°C, respectively. Under these conditions, raw rice husk moisture content is adjusted about 25% and pH around 7–8. Due to thermal decomposition characteristics of carbonate (per gram of carbonate produced 200–600 cm^3 gas), under heating, it decomposes into carbon dioxide and water in the extrude cavity and pressure is built up (at about 6–7 MPa) inside the extrude while water in the rice husk is overheated but not vaporize. When

* Corresponding author. Tel.: +86 08166089009; fax: +86 08166089009.
E-mail address: lxg-2007@163.com (X. Luo).

0304-3894/$ – see front matter.
doi:10.1016/j.jhazmat.2011.01.019

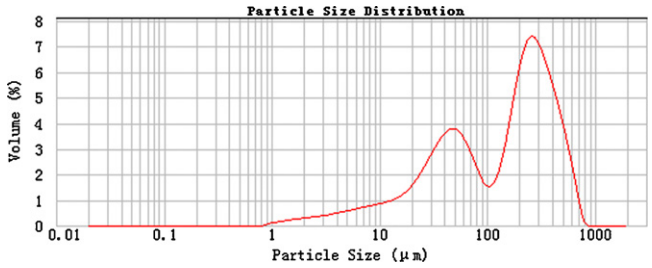

Fig. 1. Particle size distribution of the adsorbent.

overheat water in rice husk is suddenly out of extruded cavity, due to huge pressure gap between inside and outside, the water is rapidly vaporize and eject, the volume drastically increased, and the hard structure of plant fibers is cracked and loosen that the rice husk becomes crisp and porous [17,18].

The adsorbents (ERH, RRH and Coconut-shell activated carbon) are sieved through a mesh to have the uniform size for the whole study. The particle size distribution of the ERH is broadened in a range between 1 and 800 μm inclusive of two maxima at about 48 and 260 μm, respectively, as shown in Fig. 1.

The surface area and average pore diameter are determined by the Micromeritics ASAP 2010 gas adsorption surface analyzer (Delta Analytical Instruments Inc., USA), and the total pore volume is estimated as liquid volume of adsorbate adsorb at a relative pressure of 0.99. The total content of carbon, hydrogen, nitrogen and oxygen in NHBL is determined by CHNS/O analyzer (Series || CHNS/O Analyzer 2400, PerkinElmer, USA). Scanning electron microscopy (SEM, S440-Leica Cambridge Ltd. Company) analysis is carried out for the prepared adsorbents to study the surface morphology and to verify the presence of porosity. In addition, the surface functional groups of the prepared adsorbents are detected by Fourier transform infrared (FTIR) spectroscope (Nicolet-6700). The spectra are recorded 4000–400 cm^{-1}.

2.2. Chemical and instrumentation

A stock solution of Cu^{2+} is prepared by dissolving required amount of $CuSO_4$ in distilled water. All chemicals ($CuSO_4$ and Na_2CO_3) are used of analytical grade and obtained from Chengdu Kelong Chemicals Company.

Atomic absorption spectrophotometer (AAS, TA5-990) is used for Cu^{2+} measurement. A peristaltic pump (BT-100, Shanghai Huxi Instruments Company) is also used for providing constant flow of metal ions and desorbing solution in fixed bed column.

2.3. Fixed bed column study

Column experiments are conducted in a glass column with an inner diameter (ID = 3 cm) and length (L = 30 cm). The column is packed with adsorbent between two supporting layers of glass wool. The adsorbent is added from the top of the column. The metal ions solution is pumped upwards the adsorber from a liquid holding tank and a peristaltic pump that can control the inlet flow rate. The samples are collected in regular time intervals and stored for analysis. The schematic diagram of the column system is shown in Fig. 2.

2.4. Equilibrium uptake studies

The maximum column capacity, q_{total} (mg), for a given inlet concentration and flow rate is equal to the area under the plot of the adsorbed Cu^{2+} concentration C_{ad} ($C_{ad} = C_0 - C_e$, where C_e is effluent metal ions concentration and C_0 is influent metal ions concentration) (mg L^{-1}) versus time (h) and is calculated as following [19]:

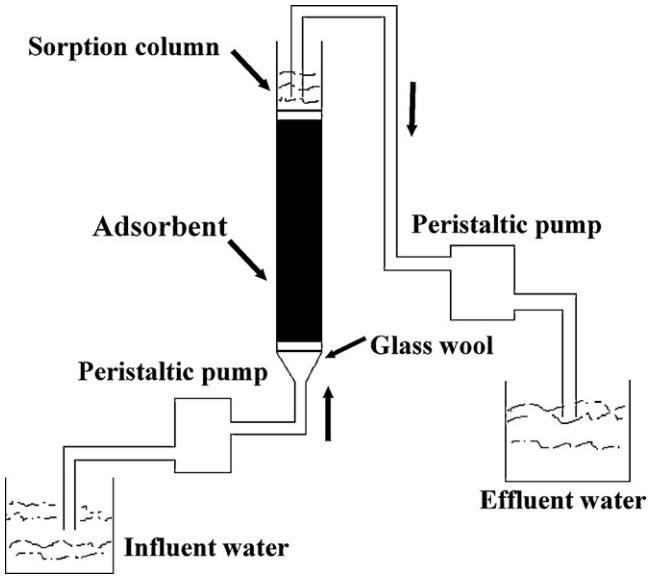

Fig. 2. Schematic diagram of lab-scale column system.

$$q_{total} = \frac{QA}{1000} = \frac{QA}{1000}\int_{t=0}^{t=t_{total}} C_{ad}\,dt \quad (1)$$

where t_{total}, Q and A are the total flow time (min), flow rate (ml min^{-1}) and the area under the breakthrough curve, respectively.

The equilibrium uptake ($q_{eq(exp)}$), the weight of Cu^{2+} adsorbed per unit dry weight of adsorbent(mg g^{-1}) in the column, is calculated as following:

$$q_{eq(exp)} = \frac{q_{total}}{X} \quad (2)$$

where X is the total dry weight of ERH in column (g).

3. Results and discussion

3.1. Characterization of rice husk

3.1.1. Pore structure and pore size distribution

The BET surface area, Langmuir surface area and average pore diameter results were presented in Table 1. The value of BET surface area of ERH (1.708 m^2 g^{-1}) was higher than RRH (0.918 m^2 g^{-1}), but lower than C-AC (743.976 m^2 g^{-1}). The low value of surface area also indicated low porosity. Pore sizes were classified in accordance with the classification adopted by the International Union of Pure and Applied Chemistry (IUPAC), that was, micropores (diameter (d) < 20 Å), mesopores (20 Å < d < 500 Å), and macropores (d > 500 Å). The average pore diameter determined by BJH method was 102.4957 Å, suggesting that ERH consists of mesopores.

Table 1
Physical characteristic of ERH, RRH and C-AC.

Parameter	ERH	RRH	C-AC
S_{BET} (m^2 g^{-1})[a]	1.708	0.918	743.976
S_L (m^2 g^{-1})[b]	2.051	1.273	1002.81
V_{tot} (cm^3 g^{-1})[c]	0.0593	0.00705	0.364
D_p (Å)[d]	102.496	140.282	19.561

[a] BET surface area.
[b] Langmuir surface area.
[c] Total pore volume.
[d] Average pore diameter.

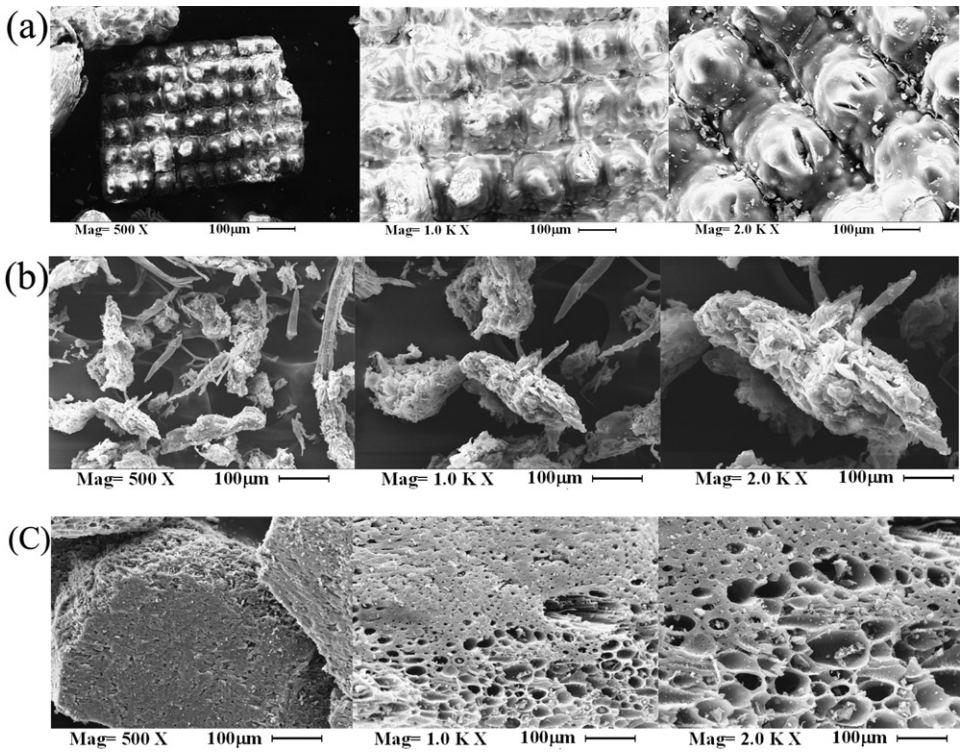

Fig. 3. SEM image of adsorbents: (a) for RRH, (b) for ERH and (c) for C-AC.

3.1.2. SEM images and FTIR spectra

The SEM images at 500×, 1000× and 2000× magnifications reveal the surface of adsorbents (RRH, ERH and C-AC) as shown in Fig. 3, and the bar in the figures indicates the magnification that were represented by the first number (in μm). As shown in Fig. 3, ERH was a porous biosorbent and had irregular structure, which favours the biosorption of Cu^{2+} on different parts of the biosorbent; ERH exhibits abundant of roughness, and more crisp compared with RRH, which might propitious to its adsorption ability; and many pores were clearly found on the surface of the C-AC, and the well-developed pores had led to the large surface area and porous structure of the C-AC.

The FTIR analysis of RRH and ERH were shown in Fig. 4, which indicated the presence of the same types of functional groups in the biosorbents. The broad band at 2923.9 cm^{-1} that represents bounded C–H groups, the bending vibration peak of $–CH_2$ and $–CH_3$ could be ascribed to the band that appeared at 1453.3 cm^{-1}, at the wave number 1055.1 cm^{-1} were also observed, the peak could be corresponded to the C–O vibration from the carbohydrate existing in the rise husk, C–O–H (898.2 cm^{-1}) [20], and –COOH (1511.9 cm^{-1}). Dominated the silica functional groups of Si–O–Si (1055.1 cm^{-1}), Si–H (798.4, 468.4 cm^{-1}) and –OH and Si–OH (3000–3700 cm^{-1}) [21].

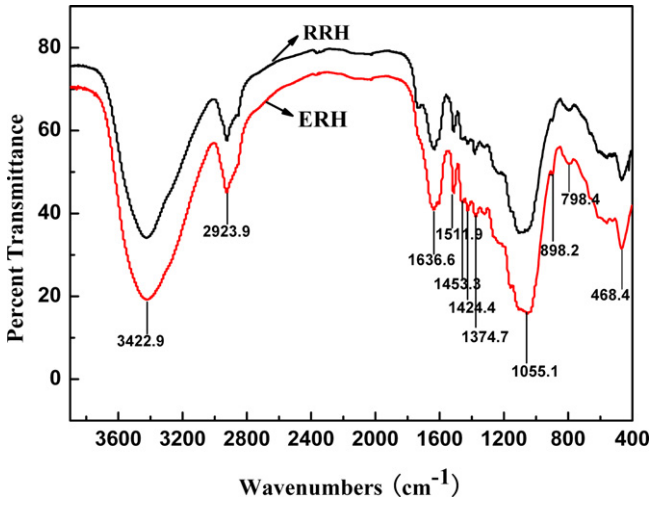

Fig. 4. FTIR spectra of RRH and ERH.

3.2. Behavior of adsorption column

As the adsorbate solution moves, adsorption zone also starts moving. After some time effluent concentration starts to rise, this is termed as breakpoint. So breakthrough time (t_a) is defined as the time required approaching a specific breakthrough concentration (10% of initial concentration C_0). The loading behavior of Cu^{2+} to be removed from solution in a fixed-bed is usually expressed in term of C_e/C_0 as a function of time, giving a breakthrough curve, and the pH of copper ions solution is 5.45 for this column experiment.

3.2.1. Effect of bed height

The breakthrough curves of copper ions adsorption obtained at different bed depths with a copper concentration of 10 mg L^{-1} at flow rate of 10 ml min^{-1} were given (Fig. 5). The bed depth of column was packed to approximately 3, 6 and 9 cm, corresponding to 5, 10 and 15 g of adsorbents (RRH and ERH). When the bed depth was reduced, axial dispersion phenomena predominated in the mass transfer and reduced the diffusion of copper ions. The copper ions did not have enough time to diffuse into the whole of the adsorbents mass [22]. As observed from Table 2, an increase of the t_a and $q_{eq(exp)}$ was noticed at the breakthrough point with an increase in bed depth. This was due to increase in the specific surface of the adsorbents which supplies more fixation binding sites. Then it followed that a delayed breakthrough of the pollutant leaded to an increase in the volume of solution treated. The increase in adsorption with that in bed depth was due to the increase in absorbents

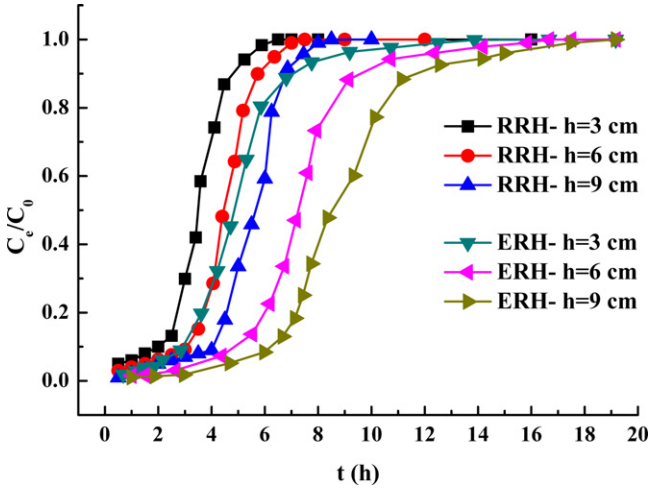

Fig. 5. Breakthrough curves of Cu^{2+} removal by RRH and ERH for different bed depth.

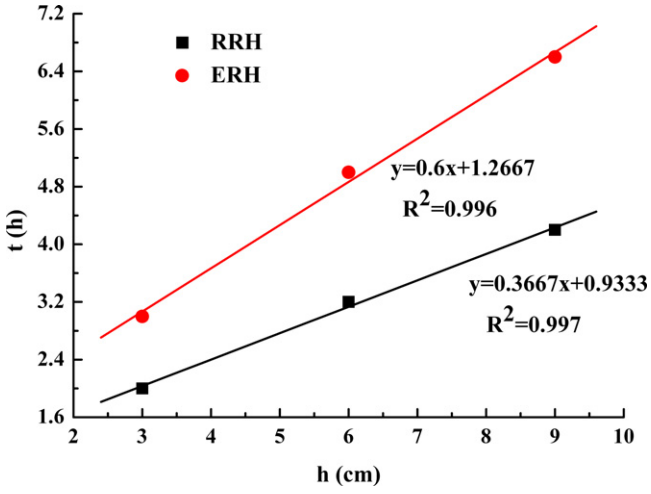

Fig. 6. BDST plot for Cu^{2+}.

doses in larger beds which provided greater surface area (or adsorption sites). The $q_{eq(exp)}$ of ERH for different bed depth 3, 6 and 9 cm, were 5.951, 4.389 and 3.54 mg g^{-1}, respectively, and the $q_{eq(exp)}$ of RRH were 4.112, 2.634 and 2.155 mg g^{-1}, respectively.

3.2.2. Bohrat–Adams model

Data collected during laboratory tests serves as the basis for the design of full-scale adsorption columns. A number of mathematical models have been developed for the use in design. Among various design approaches, bed depth service time (BDST) approach based on Bohrat–Adams equation is widely used [15,16]. This approach is referred as the BDST approach. The equation of Bohrat–Adams, which is based on surface reaction rate theory, can be represented as following:

$$t = \frac{N_0}{C_0 V} X - \frac{1}{C_0 K} \ln\left(\frac{C_0}{C_B} - 1\right) \quad (3)$$

where C_0 is the initial concentration of solute (mg L^{-1}), C_B is the desired concentration of solute at breakthrough (mg L^{-1}), K is the adsorption rate constant (L mg^{-1} h^{-1}), N_0 is the adsorption capacity (mg L^{-1}), X is the bed depth of column (cm), V is the linear flow velocity of feed to bed (cm h^{-1}), and t is the service time of column (h).

The form of the Bohrat–Adams equation, shown as Eq. (3) can be used to determine the t, for the given values of X, N_0, C_0 and K these must be determined for laboratory columns operated over a range of velocity values, V.

Setting $t = 0$ and solving Eq. (3) for X yields

$$X_o = \frac{V}{KC_0} \ln\left(\frac{C_0}{C_B} - 1\right) \quad (4)$$

Table 2
t_a and $q_{eq(exp)}$ for RRH and ERH at different parameters.

H (cm)	V (ml min)	C_0 (mg L^{-1})	t_a (h)		$q_{eq(exp)}$ (mg g^{-1})	
			RRH	ERH	RRH	ERH
3	10	10	2	3	4.112	5.951
6	10	10	3.2	5	2.634	4.389
9	10	10	4.2	6.6	2.155	3.54
9	5	10	7	12.8	2.227	3.763
9	15	10	1.5	3.4	1.427	3.005
9	10	20	2.8	4.9	3.213	5.497
9	10	50	0.9	1.833	4.094	6.333

where X_0 is the minimum column height which is necessary to produce an effluent concentration C_B, also known as critical bed depth.

At least nine individual column tests must be conducted to collect the laboratory data required for the original Bohrat–Adams approach, an expensive and time-consuming task. With the modified Bohrat–Adams equation, it only has to do three-fixed bed tests to collect the necessary data instead of nine. The Bohrat–Adams Eq. (3) can be expressed as

$$t = aX + b \quad (5)$$

where

$$a = \text{slope} = \frac{N_0}{C_0 V} \quad (6)$$

and

$$b = \text{intercept} = -\frac{1}{KC_0} \ln\left(\frac{C_0}{C_B} - 1\right) \quad (7)$$

In order to develop a BDST relation, the data of breakthrough curves plotted for each bed depth of 3, 6 and 9 cm by recording the operating time to reach a certain removal at each bed depth. The details of fitted equations between t_a and the bed depth (H) and their corresponding R^2 values were given in Fig. 6. These fitted curves which were linear could be used for predicting t_a at the given bed depth for ERH and RRH as the R^2 values > 0.99.

From the slope and intercept of the 10% saturation line design parameters like K and N_0 could be found out using Eqs. (6) and (7). The minimum column height (X_0) necessary to produce an effluent concentration C_B could be calculated by using Eq. (4). The values of K, N_0 and X_0 were found to be 0.174 L mg^{-1} h^{-1}, 509.556 mg L^{-1} and 2.104 cm for ERH, respectively, and 0.235 L mg^{-1} h^{-1}, 311.424 mg L^{-1} and 2.549 cm for RRH, respectively. At a constant flow velocity of feed, since K and N_0 were inversely proportional to X_0 and the product of K and N_0 was a unique constant for a given absorbent, a greater N_0 and a smaller X_0 indicate high efficiency for an absorption material. The N_0 was much greater and the X_0 was slightly smaller for ERH compared to RRH, indicating that both the adsorbents were highly efficient for removal of Cu^{2+} from water environment, and ERH was even more efficient.

3.2.3. Effect of flow rate

Columns ran with flow rates of 5, 10 and 15 ml min, the initial Cu^{2+} concentration was kept constant at 10 mg L^{-1} and the bed height was 9 cm. As shown from the breakthrough curves in Fig. 7,

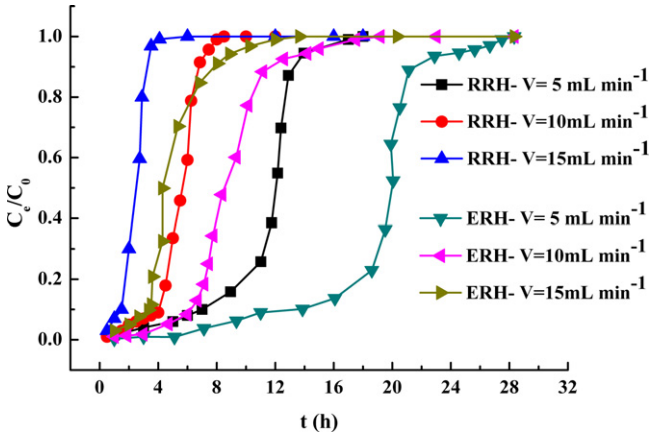

Fig. 7. Breakthrough curves of Cu^{2+} removal by RRH and ERH for different flow rate.

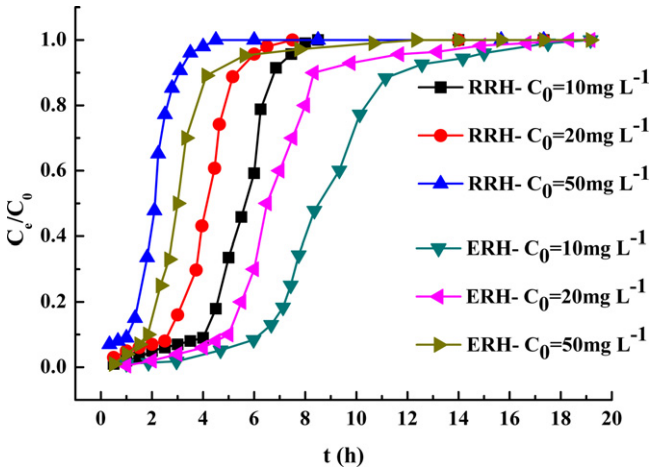

Fig. 8. Breakthrough curves of Cu^{2+} removal by RRH and ERH for different concentration.

flow rate had great influence on the metal uptake capacity, and the detail of t_a and $q_{eq(exp)}$ was given in Table 2, the t_a and $q_{eq(exp)}$ decreased with the increase in flow rates. Lower flow rates result in high residence times in the column. It was well known that because of the relatively slow loading kinetics of the absorbent, relatively long residence times were needed. In actual column operation, any volume element of the solution was in contact with a given layer of the bed for only a limited period of time, usually insufficient for attainment of equilibrium. Thus the failure of attaining local equilibrium results in lower uptake of copper ions from the influent solution [23].

An increased in the flow rate reduced the volume treated efficiently until breakthrough point and therefore decreased the service time of the bed. This was due to decrease in contact time between the metal ions and the absorbents at higher linear flow rates. At a higher linear flow rate, the adsorbent got saturated early, certainly because of a reduced contact time, a larger amount of copper ions were adsorbed on the absorbents and there was a weak distribution of the liquid into the column, which leads to a lower diffusivity of the solute amidst the particles of the absorbents. This showed an increase in the uptake of the metal ions due to the intra particulate phenomena [22]. The $q_{eq(exp)}$ of ERH for tested flow rates of 5, 10 and 15 ml min^{-1} were 3.763, 3.54 and 3.005 mg g^{-1}, respectively, and the $q_{eq(exp)}$ of RRH were 2.227, 2.155 and 1.427 mg g^{-1}, respectively.

3.2.4. Effect of initial concentration

The effect of initial influent concentration was investigated using synthetic solution containing 20 and 50 mg L^{-1} of copper ions (whereas original copper concentration was 10 mg L^{-1}). From Fig. 8, it showed the effect of initial concentration on the breakthrough curves by using a bed depth of 9 cm at a flow rate of 10 ml min^{-1}. A rose in the inlet metal concentration reduced the treated volume before the fixed bed adsorption bed gets saturated, a high metal concentration may saturate the absorbents more quickly, thereby decreasing the service times (t_a). Also, it was clear that the $q_{eq(exp)}$ decreased with the increase in the initial concentration (Table 2). To tested different initial concentration, the $q_{eq(exp)}$ of ERH at 10, 20 and 50 mg L^{-1} Cu^{2+} concentrations were 3.54, 5.497 and 6.333 mg g^{-1}, respectively, and the $q_{eq(exp)}$ of RRH were 2.155, 3.213 and 4.094 mg g^{-1}.

Decreasing the fed Cu^{2+} concentration increases the treated volume of feed metal concentration that could be processed, and shifts the breakthrough curves to the right. The driving force for adsorption was the concentration difference between the solute on the absorbent and the solute in the solution. A high concentration difference provided a high driving force for the adsorption process and this might explain why higher adsorption capacities were achieved in the column fed with a higher Cu^{2+} concentration. The relatively low Cu^{2+} retention for adsorbents could be attributed to the difference in the surface morphology. Adsorbent particles did not have many micropores or macropores, so its low surface area also resulted in lower sorption capacity [24].

As seen in Table 2, at different parameters the t_a and $q_{eq(exp)}$ of ERH were longer and higher when compared to that of RRH. The increase in the metal uptake capacity for the ERH was due to the increase in the surface area and pores of adsorbent that result in more binding site for the adsorption.

3.3. ERH vs. coconut-shell activated carbon

Since its first introduction for heavy metal removal, activated carbon had been shown undoubtedly as the most popular and widely used adsorbent in wastewater treatment applications throughout the world. Coconut-shell activated carbon (C-AC) with developed pore structure, high adsorption capacity, strength, chemical stability and durability, it was widely used in water treatment. Green Resources Activated Carbon Co., Ltd. provided the C-AC (special for water treatment) for this experiment, and the maximum adsorption capacity for C-AC was 1010 mg g^{-1}.

Investigation was carried out under the condition of the flow rate kept at 10 ml min^{-1}, the adsorbent dosage of 10 g and the initial copper concentration of 9.73 and 26.95 mg L^{-1}, respectively. From the results obtained by the columns experiments for ERH and C-AC, the breakthrough curves were plotted for copper ions and were shown in the Fig. 9, and the details of $q_{eq(exp)}$ were given in Table 3. It could be observed that t_a of adsorption with ERH was more, and the $q_{eq(exp)}$ of copper ions for ERH was higher when compared to that of C-AC. From Fig. 3 and Table 1, it could be seen that C-AC had more pores and larger surface area than ERH, thus, the higher metal uptake capacity for the ERH was due to adequate functional groups in the surface charge of the adsorbent, which provided more binding site for the adsorption. It could be inferred that the essential mechanism of adsorption in this case was by chemisorptions.

3.4. Column regeneration and re-usage

In order to achieve the adsorbent recycling, the performance of fixed bed column was studied for repeating adsorption–desorption cycle experiment. Desorption was carried out by using 0.01 mol L^{-1} HCl solution through the bed in the upwards flow direction at a flow rate of 8 ml min^{-1}, slightly less than the sorption flow rate

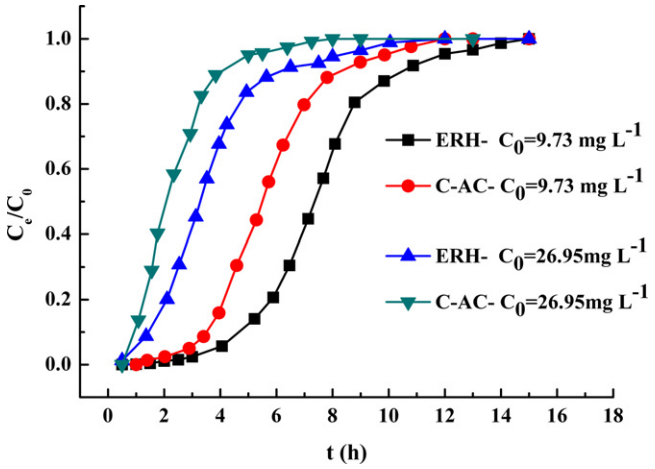

Fig. 9. Breakthrough curves for Cu^{2+} with ERH, RRH and C-AC.

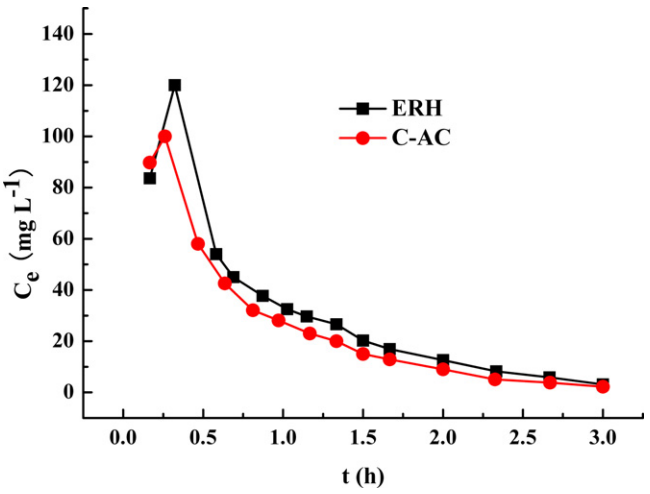

Fig. 11. Elution curves for copper ions from ERH and C-AC column.

Table 3
The t_a and $q_{eq(exp)}$ for ERH and C-AC.

Initial concentration (mg L^{-1})	t_a (h)		$q_{eq(exp)}$ (mg g^{-1})	
	ERH	C-AC	ERH	C-AC
9.73	5.2	3.6	4.357	3.319
26.95	1.5	0.8	5.838	4.103

10 ml min^{-1}, so that volume of regenerant was less which helps in easy handling and high in concentration so that economical metal ion recovery was possible. Then, the desorbed column was washed with 800 ml distilled water at a flow rate of 25 ml min^{-1} and then by reactivation with 0.01 mol L^{-1} NaOH with a flow rate of 10 ml min^{-1} and finally washed it again with 800 ml distilled water at a flow rate of 25 ml min^{-1}, all in upwards flow direction of the column.

The columns experiments for ERH and C-AC with a bed depth of 9 cm, a metal ion concentration of 10 mg L^{-1} and a flow rate of 10 ml min^{-1}, the details of cycles and $q_{eq(exp)}$ were shown in Fig. 10. It was observed that, under the same conditions, the $q_{eq(exp)}$ of ERH column had not been reduced significantly, until the sixth cycle. On the contrary, after NaOH activation, the $q_{eq(exp)}$ or say adsorption capacity had increased compared to the first cycle. But since from the seventh cycle, the adsorption capacity decreased, until

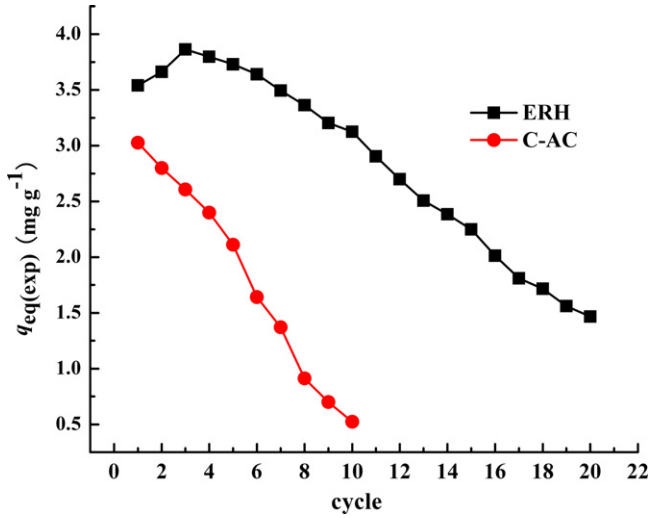

Fig. 10. Adsorption–desorption cycles and $q_{eq(exp)}$ for Cu^{2+} with ERH and C-AC.

20th cycle reduced to 42.46% of the first. But, the $q_{eq(exp)}$ of C-AC column Sharp decline, at 10th cycle reduced to 17.31% of the first.

The mineral acids were proton-exchange agents, which dislodge high valance metal ions from biomass [25]. Excessive amount of H^+ could reduce the metal sorptive capacity. Washing the biomass with deionized water could remove H^+ and could be regenerated. Yan and Viraraghavan [25] observed similar phenomena and indicated that biomass could be repeatedly subjected to alkaline treatment without losing its adsorption properties. Because NaOH was capable to remove the lipids, proteins and some soluble polysaccharide which contained in ERH and might change the surface chemistry and physical state, consequently, the cell wall structure may become more loosely, more voids and surface areas available to absorbate, resulting in increase of the adsorption capacity of Cu^{2+}.

The concentration of Cu^{2+} outflow from the desorption-column was monitored after different time interval as shown in Fig. 11. It was observed that desorption cycle took 1.333 h, after the further desorption was negligible, the total volume of this eluent at 3 h was 1440 ml. The maximum concentration of Cu^{2+} from the ERH and C-AC desorption-column were obtained at about contact time of 20 and 15 min, respectively. The eluting solution was lower in volume and higher in concentration, which could help in easy handling, recovery and reuse of Cu^{2+}. It was illustrated that Cu^{2+} was easily desorbed using HCl solution, and more than 85% of copper ions were recovered. Therefore, copper ions were easily recovered and reused and the adsorbents (ERH and C-AC) could be then handled and reused repeatedly.

3.5. Adsorption mechanisms

Rice husk included cellulose, hemicellulose, lignin, Water, Mineral ash, etc. Cellulose, and lignin contained a large amount of hydroxyl, and the chemical formulas were shown in Fig. 12. FTIR (Fourier Transform Infrared), XPS (X-ray photoelectron spectra), among others, had been used to determine functional groups and at the same time to elucidate the biosorbents metal sorption mechanism [26]. From the FTIR of ERH, some of the functional groups had been identified in ERH including: carboxyl, hydroxyl and phenolic (from Fig. 12).

A series of batch adsorption experiments were conducted at different initial copper concentrations and initial pH values of 5.45. When the adsorption reached equilibrium, it was found that pH_e (equilibrium pH) values were lower than corresponding pH_0 (initial

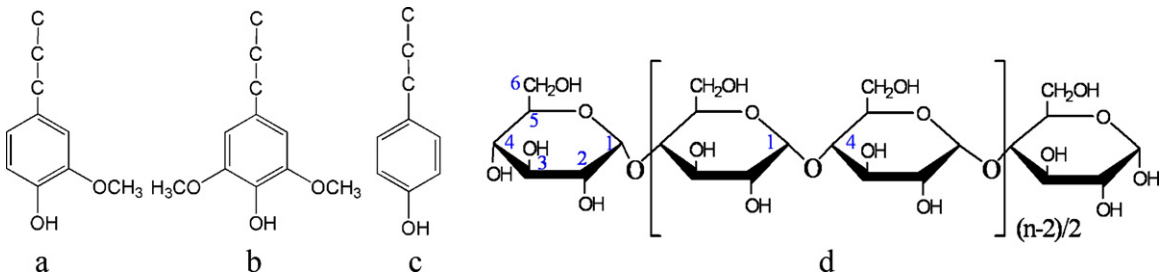

Fig. 12. The chemical formulas of lignin and cellulose: (a), (b), (c) for the basic chemical phenyl propane units of lignin; (d) for cellulose.

pH) values, which indicates that copper ions were adsorbed onto adsorbent from the liquid phase along with H^+ ions removal.

Larous et al. [27] established that the maximum sorption efficiency in the pH range of 2–8 may be due to the interaction of Cu^{2+}, $Cu(OH)^+$, $Cu(OH)_2$ with surface functional groups (–ROH). Yu et al. [28] proposed that H^+ ions (present in carboxyl and phenolic groups of maple sawdust) could be exchanged with metal cations in solution. So, the uptake of bivalent cooper by ERH was coupled with a release of protons from the carboxyl and hydroxyl groups, at pH 5.45 there were three species present in solution as suggested by [29]. Cu^{2+} in very small quantity and $Cu(OH)^+$ and $Cu(OH)_2$ in large quantities, and the following ion exchange was proposed as the copper sorption mechanism:

$$2\{\equiv R\text{–}COOH\} + Cu^{2+} \leftrightarrow \{\equiv R\text{–}COOH\}_2\text{–}Cu + 2H^+ \quad (8)$$

$$\{\equiv R\text{–}COOH\} + Cu(OH)^+ \leftrightarrow \{\equiv R\text{–}COO\}\text{–}CuOH + H^+ \quad (9)$$

$$2\{\equiv R\text{–}OH\} + Cu^{2+} \leftrightarrow \{\equiv R\text{–}O\}_2\text{–}Cu + 2H^+ \quad (10)$$

$$\{\equiv R\text{–}OH\} + Cu(OH)^+ \leftrightarrow \{\equiv R\text{–}O\}\text{–}CuOH + H^+ \quad (11)$$

$$\{\equiv R\text{–}COOH\} + Cu(OH)_2 \leftrightarrow \{\equiv R\text{–}COO\}Cu(OH)_2H \quad (12)$$

$$\{\equiv R\text{–}OH\} + Cu(OH)_2 \leftrightarrow \{\equiv R\text{–}O\}Cu(OH)_2H \quad (13)$$

where R represented the immobile functional anion group attached to the exchangeable proton.

These species were adsorbed at the surface of ERH by ion exchange mechanism with the functional groups present in ERH as shown reactions (8)–(11), reactions (12) and (13) were shown by hydrogen bonding. Ion exchange and hydrogen bonding had been identified as the main mechanism involved in the binding of copper ions on ERH.

4. Conclusion

ERH was found to be an effective adsorbent for removal of copper ions. From the study on adsorption of Cu^{2+} in different column design parameters, we have found the removal of Cu^{2+} from aqueous solutions depends strongly on bed depth, flow rate and initial concentration. As expected from Bohrat–Adams model, the experimental data were well fitted by Bohrat–Adams model. The performances of ERH and C-AC columns were also studied for adsorption–desorption cycles, respectively. Desorption of Cu^{2+} was possible using HCl solution. The activated and regenerated column adsorption capacity increased in ERH after re-activation using NaOH. But, the adsorption capacity of C-AC column sharp declined. From the concentrations of cooper ions in eluants for columns, more than 85% of copper ions were recovered. Therefore, copper ions were easily desorbed from the ERH and C-AC columns using HCl solution. Among RRH, ERH and C-AC as column filling absorbents, ERH showed significantly higher adsorption capacity of metal ions. Ion exchange and hydrogen bonding were the major mechanism of retention of copper by ERH, and showing a high efficiency.

Acknowledgement

This work was supported by National Key Technology R&D Program of China (No. 2007BAB18808).

References

[1] W.Y. Shi, H. Shao, H. Li, et al., Progress in the remediation of hazardous heavy metal-polluted soils by natural zeolite, J. Hazard. Mater. 170 (2009) 1–6.
[2] P.J. Li, X. Wang, G. Allinson, et al., Risk assessment of heavy metals in soil previously irrigated with industrial wastewater in Shenyang, China, J. Hazard. Mater. 161 (2009) 516–521.
[3] X.W. Lu, L.J. Wang, K. Lei, et al., Contamination assessment of copper, lead, zinc, manganese and nickel in street dust of Baoji, NW China, J. Hazard. Mater. 161 (2009) 1058–1062.
[4] J. Sunarso, S. Ismadji, Decontamination of hazardous substances from solid matrices and liquids using supercritical fluids extraction: a review, J. Hazard. Mater. 161 (2009) 1–20.
[5] J.F. Peng, Y.H. Song, P. Yuan, et al., The remediation of heavy metals contaminated sediment, J. Hazard. Mater. 161 (2009) 633–640.
[6] W. Liu, Y.S. Yang, P.J. Li, et al., Risk assessment of cadmium-contaminated soil on plant DNA damage using RAPD and physiological indices, J. Hazard. Mater. 161 (2009) 878–883.
[7] C.C. Tung, Y.M. Yang, C.H. Chang, et al., Removal of copper ions and dissolved phenol from water using micellar-enhanced ultra. Ultration with mixed surfactants, J. Waste Manage. 22 (2002) 695–701.
[8] A. Kapoora, T. Viraraghavan, Removal of heavy metals from aqueous solutions using immo-bilized fungal biomass in continuous mode, J. Water Resour. 6 (1998) 1968–1977.
[9] D.S. Kim, The removal by crab shell of mixed heavy metal ions in aqueous solution, J. Bioresour. Technol. 87 (2003) 55–357.
[10] S. Babel, T.A. Kurniawan, Low-cost adsorbents for heavy metals uptake from contaminated water: a review, J. Hazard. Mater. B 97 (2003) 219–243.
[11] J. Wang, X. Zhan, D. Ding, D. Zhou, Bioadsorption of lead (II) from aqueous solution by fungal biomass of Aspergillus niger, J. Biotechnol. 87 (2001) 273–277.
[12] G. Wu, H. Kang, X. Zhang, et al., A critical review on the bio-removal of hazardous heavy metals from contaminated soils: Issues, progress, eco-environmental concerns and opportunities, J. Hazard. Mater. 174 (2010) 1–8.
[13] B. Wei, L. Yang, A review of heavy metal contaminations in urban soils, urban road dusts and agricultural soils from China, Microchem. J. 94 (2010) 99–107.
[14] S. Nayek, S. Gupta, R.N. Saha, Metal accumulation and its effects in relation to biochemical response of vegetables irrigated with metal contaminated water and wastewater, J. Hazard. Mater. 178 (2010) 588–595.
[15] U. Kumar, M. Bandyopadhyay, Fixed bed column study for Cd (II) removal from wastewater using treated rice husk, J. Hazard. Mater. B 129 (2006) 253–259.
[16] S. Mohan, G. Sreelakshmi, Fixed bed column study for heavy metal removal using phosphate treated rice husk, J. Hazard. Mater. 153 (2008) 75–82.
[17] Xue-gang Luo, Carbonate in the extrusion rice husk of the application process, J. Agric. Eng. 14 (1998) 235–239.
[18] Xue-gang Luo, Plant crude fiber breaker and its use, P. China Patent: ZL97107538.7;
F.U. Richard, K.L. Shuttleworth, Curr. Opin. Biotechnol. 7 (1996) 307–310.
[19] E. Malkoc, Y. Nuhoglu, Removal of Ni (II) ions from aqueous solutions using waste of tea factory: adsorption on a fixed-bed column, J. Hazard. Mater. B 135 (2006) 328–336.
[20] M.S. Solum, R.J. Pugmire, M. Jagtoyen, F. Derbyshire, Evolution of carbon structure in chemically activated wood, Carbon 33 (1995) 1247–1254.
[21] T.H. Liou, Preparation and characterization of nano-structured silica from rice husk, Mater. Sci. Eng. A364 (2004) 313–323.
[22] V.C. Taty-Costodes, H. Henri Fauduet, C. Catherine Porte, Y.S. Ho, Removal of lead(II) ions from synthetic and real effluents using immobilized Pinus sylvestris sawdust: adsorption on a fixed-bed column, J. Hazard. Mater. B 123 (2005) 135–144.
[23] V.J. Inglezakis, H. Grigoropoulou, Effects of operating conditions on the removal of heavy metals by zeolite in fixed bed reactors, J. Hazard. Mater. B 112 (2004) 37–43.

[24] Z. Aksu, F. Gönen, Biosorption of phenol by immobilized activated sludge in a continuous packed bed: prediction of breakthrough curves, Process Biochem. 39 (2004) 599–613.
[25] G. Yan, T. Viraraghavan, Heavy metal removal from aqueous solution by fungus Mucor rouxii, Water Res. 37 (2003) 4486–4496.
[26] K.K. Krishnani, X.G. Meng, C. Christodoulatos, V.M. Boddu, Biosorption mechanism of nine different heavy metals onto biomatrix from rice husk, J. Hazard. Mater. 153 (3) (2008) 1222–1234.
[27] S. Larous, A.-H. Meniai, M. Bencheikh Lehocine, Experimental study of the removal of copper from aqueous solutions by adsorption using sawdust, Desalination 185 (2005) 483–490.
[28] L.J. Yu, S.S. Shukla, K.L. Dorris, A. Shukla, J.L. Margrave, Adsorption of chromium from aqueous solutions by maple sawdust, J. Hazard. Mater. 100 (1–3) (2003) 53–63.
[29] H.A. Elliot, C.P. Huang, The adsorption of Cu (II) complexes onto aluminosilicates, Water Res. 15 (7) (1981) 849–855.